Properties of $Q\bar{Q}$ mesons in nonrelativistic QCD formalism

Ajay Kumar Rai,[1,*] Bhavin Patel,[2] and P. C. Vinodkumar[2]
[1]*Physics Section, Applied Sciences and Humanities Department*
Sardar Vallabh National Institute of Technology, Surat-395 007, Gujarat, India
[2]*Department of Physics, Sardar Patel University, Vallabh Vidyanagar, Anand 388 120, Gujarat, India*
(Received 8 June 2007; revised manuscript received 21 August 2008; published 11 November 2008)

The decay rates of $Q\bar{Q}$ mesons ($Q\, \varepsilon\, c, b$) are studied in the nonrelativistic quantum chromodynamics (QCD) formalism in terms of their short-distance and long-distance coefficients. The long-distance coefficients are obtained through phenomenological potential model description of the mesons. The model parameters that reproduces the mass spectrum of the $c\bar{c}$, $b\bar{b}$, and $c\bar{b}$ mesons are employed to study the decay widths of these mesons. We extract the mass spectrum and the respective radial wave functions from the different potential models as well as from a nonrelativistic phenomenological quark-antiquark potential of the type $V(r) = -\frac{\alpha_c}{r} + Ar^{\nu}$, with ν varying from 0.5 to 2. The spin hyperfine and spin-orbit interactions are employed to obtain the masses of the pseudoscalar and vector mesons. The decay constants with QCD corrections are computed in this model as well as in the case of other potential models for comparison. The digamma and dileptonic decays of $c\bar{c}$ and $b\bar{b}$ mesons are investigated using some of the known potential models without and with radiative corrections up to the lowest order. These decay width are also computed within the nonrelativistic QCD formalism up to $O(v^4)$ by making uses of the respective spectroscopic parameters of the models. Our theoretical predictions of the decays of the $c\bar{c}$ and $b\bar{b}$ mesons and the results obtained from some of the other potential schemes are compared with the experimental values. The partial widths and lifetime of the B_c meson are also computed using the model parameters and are found to be in good accordance with the experimental values.

DOI: 10.1103/PhysRevC.78.055202 PACS number(s): 12.39.Jh, 12.40.Yx, 13.20.Gd, 13.20.Fc

I. INTRODUCTION

Recently, there have been renewed interest in the spectroscopy of the heavy flavored hadrons due to the number of experimental facilities (CLEO, DELPHI, Belle, BaBar, LHCb, etc.) that have been continuously providing and expected to provide more accurate and new information about the hadrons from light flavor to heavy flavor sectors [1,2].

The heavy flavor mesons are those in which at least one of the quark or antiquark or both the quark and antiquark belong to a heavy flavor sector; particularly the charm or beauty. They are represented by $Q\bar{Q}$ mesonic systems that include the quarkonia ($c\bar{c}$ and $b\bar{b}$) and B_c ($b\bar{c}$ or $c\bar{b}$) mesons. The investigation of the properties of these mesons gives very important insight into heavy quark dynamics. Heavy quarkonia have a rich spectroscopy with many narrow states lying under the threshold of open flavor production [3,4].

The success of theoretical model predictions with experiments can provide important information about the quark-antiquark interactions. Such information is of great interest, as it is not possible to obtain the $Q\bar{Q}$ potential starting from the basic principle of quantum chromodynamics (QCD) at the hadronic scale. In this scale it is necessary to account for nonperturbative effects connected with complicated structure of QCD vacuum. All this led to a theoretical uncertainty in the $Q\bar{Q}$ potential at large and intermediate distances. It is just in this region of large and intermediate distances that most of the basic hadron resonances are formed. Among many theoretical attempts or approaches to explain the hadron properties based on its quark structure very few were successful in predicting the hadronic properties starting from mass spectra to decay widths. For the mass predictions, the nonrelativistic potential models with Buchmüller and Tye [5], Martin [6–8], Log [9,10], Cornell [11], etc., were successful at the heavy flavor sectors, whereas the Bethe-Salpeter approach under harmonic confinement [12] was successful at light flavor sectors. There exist relativistic approaches for the study of the different hadronic properties [13,14]. The nonrelativistic potential model has been successful for ψ and Υ families, whereas the relativistic approaches yield better results in the lighter sector. Some potential models have also predicted the masses and various decays of the heavy-heavy mesons that are in fair agreement with the experimental results [15–24]. A comprehensive review of developments in heavy quarkonium physics is available in Ref. [25]. The new role of the heavy flavor studies as the testing ground for the nonperturbative aspects of QCD demands extension of earlier phenomenological potential model studies on quarkonium masses to their predictions of decay widths with the nonperturbative approaches like nonrelativistic QCD (NRQCD).

The decay rates of the heavy-quarkonium states into photons and pairs of leptons are among the earliest applications of perturbative QCD [26,27]. In these analyses, it was assumed that the decay rates of the meson factored into a short-distance part that is related to the annihilation rate of the heavy quark and antiquark and long-distance factors containing all nonperturbative effects of the QCD. The short-distance factor, calculated in terms of the running coupling constant $\alpha_s(m_Q)$ of QCD, was evaluated at the scale of the heavy-quark mass m_Q, whereas the long-distance factor was expressed in terms of the meson's nonrelativistic wave function, or its derivatives,

*raiajayk@rediffmail.com

evaluated at origin. In case of S-wave decays [28–31] and in case of P-wave decays into photons [32], the factorization assumption was supported by explicit calculations at next-to-leading-order in α_s. However, no general argument advanced for its validity in higher orders of perturbation theory. These divergence cast a shadow over applications of perturbative QCD to the calculation of annihilation rates of the heavy quarkonium states.

In this context, an elegant effort was provided by the non-relativistic QCD formalism [33]. It consists of a nonrelativistic Schrodinger field theory for the heavy quark and antiquark that is coupled to the usual relativistic field theory for light quarks and gluons. NRQCD not only organize calculation of all orders in α_s but also elaborate systematically the relativistic corrections to the conventional formula. Furthermore, it also provides nonperturbative definitions of the long-distance factors in terms of matrix elements of NRQCD, making it possible to evaluate them in the numerical lattice calculations. Analyzing S-wave decays within this frame work, it recovers, at leading order in v^2, standard factorization formulas, which contain a single nonperturbative parameter. At next-to-leading-order in v^2, the decay rates satisfy a more general factorization formula, which contains two additional independent nonperturbative matrix elements related to their radial wave functions.

Our attempt in this article would be then to study the heavy-heavy flavor mesons in the charm and beauty sector in a general frame work of the potential models. The model parameters used for the predictions of the masses and their radial wave functions would be used for the study of their decay properties using NRQCD formalism.

For completion, we present a detail analysis of mass spectra of $c\bar{c}$, $c\bar{b}$, and $b\bar{b}$ mesons in the potential scheme of coulomb plus power potential (CPP$_\nu$) with the power index (ν), varying from 0.5 to 2. Spin hyperfine and spin-orbit interactions are introduced to get the S-wave and P-wave masses of the pseudoscalar and vector mesons. We present details of the nonrelativistic treatment of the heavy quarks along with the computed results in Sec. II. The decay constants $f_{P,V}$ of these mesons incorporating QCD corrections up to $O(\alpha_s)$ are presented in Sec. III. The weak decay of the B_c meson and its life time is computed in Sec. IV, whereas in Sec. V we present details of the computations of the di-γ decays of pseudoscalar states and the leptonic decay widths of the vector states of the $c\bar{c}$ and $b\bar{b}$ quarkonia in the framework of the NRQCD formalism as well as other treatments incorporating different correction terms to the respective decay widths. Though the NRQCD formalism takes advantage of the fact that heavy quark mass is much larger than the other energy scales such as the binding energy scale, $\Lambda_{\rm QCD}$ and $|\vec{p}|$, the energy fluctuations of the heavy quarks of the order of the light energy scale are implemented in potential NRQCD [34–36]. A comprehensive comparison of the results are presented in this section. Finally, we draw our conclusions in Sec. VI.

II. NONRELATIVISTIC TREATMENT FOR $Q\bar{Q}$ SYSTEMS

Even though there are attempts based on the relativistic theory like the light front approach for the study of the heavy flavored quarks, under nonrelativistic approximations, they reproduce the results of the nonrelativistic quark-potential models [37]. In the center of mass frame of the heavy quark-antiquark system, the momenta of quark and anti-quark are dominated by their rest mass $m_{Q,\bar{Q}} \gg \Lambda_{\rm QCD} \sim |\vec{p}|$, which constitutes the basis of the nonrelativistic treatment. In NRQCD, the velocity of heavy quark is chosen as the expansion parameter [38].

Hence, for the study of heavy-heavy bound state systems such as $c\bar{c}$, $c\bar{b}$, and $b\bar{b}$, we consider a nonrelativistic Hamiltonian given by [21–23]

$$H = M + \frac{p^2}{2m} + V(r), \tag{1}$$

where

$$M = m_Q + m_{\bar{Q}}, \quad \text{and} \quad m = \frac{m_Q m_{\bar{Q}}}{m_Q + m_{\bar{Q}}}, \tag{2}$$

where m_Q and $m_{\bar{Q}}$ are the mass parameters of quark and antiquark, respectively, p is the relative momentum of each quark, and $V(r)$ is the quark-antiquark potential. Though linear plus coulomb potential is a successful well-studied nonrelativistic model for the heavy flavor sector, their predictions for decay widths are not satisfactory due to the improper value of the radial wave function at the origin compared to other models [22]. Recently, we have considered a general power potential with color coulomb term of the form

$$V(r) = \frac{-\alpha_c}{r} + Ar^\nu \tag{3}$$

as the static quark-antiquark interaction potential (CPP$_\nu$). Here, for the study of mesons, $\alpha_c = \frac{4}{3}\alpha_s$, where α_s is the strong running coupling constant, A is the potential parameter, and ν is a general power such that the choice $\nu = 1$ corresponds to the coulomb plus linear potential. This potential belong to the special choices of the generality of the potentials, $V(r) = -Cr^\alpha + Dr^\beta + V_0$ [39–41] with $V_0 = 0$ $\alpha = -1$, $\beta = \nu$. Choices of the power index in the range $0.5 \leqslant \nu \leqslant 2.0$ have been explored for the present study. The different choices of ν here, correspond to different potential forms. Thus, the potential parameter A can also be different numerically and dimensionally for each choices of ν. The properties of the light-heavy flavour mesons have been calculated using the Gaussian trial wave function [21]. Masses and decay constant of the light-heavy systems are found to be in agreement with the experimental results for the choice of $\nu \approx 0.5$. However, in the case of heavy-heavy systems the predictions of the masses were satisfactory but the decay constants and decay rates were not predicted satisfactorily [22]. Hence for the present study of heavy-heavy flavor mesons, we employ the exponential trial wave function of the hydrogenic type to generate the Schrödinger mass spectra. Within the Ritz variational scheme using the trial radial wave function we obtain the expectation values of the Hamiltonian as ($\langle H \rangle = E(\mu, \nu)$)

$$E(\mu, \nu) = M + \frac{\mu^2}{8m} + \frac{1}{2}\left[-\mu\alpha_c + A\,\frac{\Gamma(\nu+3)}{\mu^\nu}\right]. \tag{4}$$

Equation (4) gives the spin average mass of the ground state. For excited states the trial wave function is multiplied by an appropriate orthogonal polynomial function such that the excited trial wave function gets orthonormalized. So it is straightforward to assume the trial wave function for the (n, l) state to be the form given by the hydrogenic radial wave function,

$$R_{nl}(r) = \left[\frac{\mu^3(n-l-1)!}{2n(n+l)!}\right]^{1/2} (\mu r)^l e^{-\mu r/2} L_{n-l-1}^{2l+1}(\mu r). \quad (5)$$

Here, μ is the variational parameter and $L_{n-l-1}^{2l+1}(\mu r)$ is Laguerre polynomial. For a chosen value of ν, the variational parameter, μ is determined for each state using the virial theorem

$$\left\langle \frac{P^2}{2m} \right\rangle = \frac{1}{2}\left\langle \frac{rdV}{dr} \right\rangle \quad (6)$$

As the interaction potential assumed here does not contain the spin-dependent part, Eq. (4) gives the spin average masses of the system in terms of the power index ν. The spin average mass for the ground state is computed for the values of ν from 0.5 to 2. We have taken the quark mass parameters $m_b = 4.66$ GeV and $m_c = 1.31$ GeV. The potential parameter A is fixed for each choice of ν so as to get the experimental ground state masses of $c\bar{c}$, $c\bar{b}$, and $b\bar{b}$ mesons. The parameters and the fitted values of A for different systems are listed in Table I. The experimental spin average masses are computed from the experimental masses of the pseudoscalar and vector mesons using the relation,

$$M_{\mathrm{SA}} = M_P + \tfrac{3}{4}(M_V - M_P). \quad (7)$$

For the nJ state, we compute the spin average or the center-of-weight mass from the respective experimental values as

$$M_{\mathrm{CW},nJ} = \frac{\sum_J 2(2J+1)M_{nJ}}{\sum_J 2(2J+1)}. \quad (8)$$

The fitted value of A for each case of the power index ν along with other model parameters are tabulated in Table I for $c\bar{c}$, $c\bar{b}$, and $b\bar{b}$ systems. The ground-state center-of-weight masses of 3.068 GeV, 6.320 GeV, and 9.453 GeV are used to fit the A values for $c\bar{c}$, $c\bar{b}$, and $b\bar{b}$ systems, respectively. The values of $A(\nu)$ thus obtained for each case of mesonic systems are then used to predict the higher S- and P-wave masses (see Tables II–VII). The fitted values of A for each ν in the case of the heavy-heavy flavour mesons are plotted in Fig. 1. It is interesting to note that all the three plots intersect each other at ν equal to 1.1 at the value of the parameter A around 0.151 GeV$^{\nu+1}$. It can also be seen that the parametric values of A for $c\bar{c}$ and $c\bar{b}$ systems are close to each other, whereas in the case of $b\bar{b}$, they are distinctly different except at $\nu = 1.1$. It reflects the fact that potential parameter A becomes independent of the distinct energy scales of these heavy mesons at around $\nu = 1.1$.

In the case of $c\bar{c}$ and $c\bar{b}$ systems, the values of the parameter A are numerically very close to each other in the range of potential index 0.9 to 1.3. The predicted masses are also found to be in good agreement with the existing experimental states in range of power index 0.9 to 1.3 of the potential. Figure 2 shows the behavior of $|R_{1S}(0)|$ with the potential index ν for all the three ($c\bar{c}$, $c\bar{b}$, and $b\bar{b}$) mesons. Like other potential model predictions of the wave functions (at the origin) of $b\bar{c}$ system lie in between those of $c\bar{c}$ and $b\bar{b}$ systems. We obtained

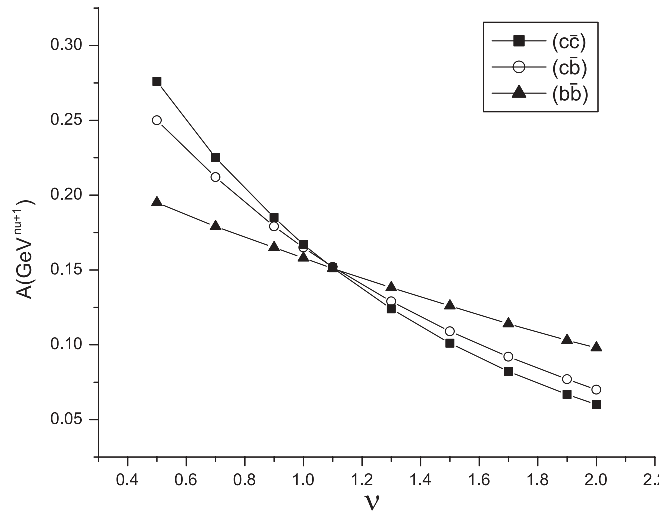

FIG. 1. Fitted potential parameter A against potential index ν.

TABLE I. Potential parameters A (GeV$^{\nu+1}$) and α_c.

ν	A ($c\bar{c}$)	A ($b\bar{c}$)	A ($b\bar{b}$)
0.5	0.276	0.250	0.195
0.7	0.225	0.212	0.179
0.9	0.185	0.179	0.165
1.0	0.167	0.165	0.158
1.1	0.151	0.152	0.151
1.3	0.124	0.129	0.138
1.5	0.101	0.109	0.126
1.7	0.082	0.092	0.114
1.9	0.067	0.077	0.103
2.0	0.060	0.070	0.098

$\alpha_c(c\bar{c}) = 0.40$, $\alpha_c(b\bar{c}) = 0.34$, $\alpha_c(b\bar{b}) = 0.30$,

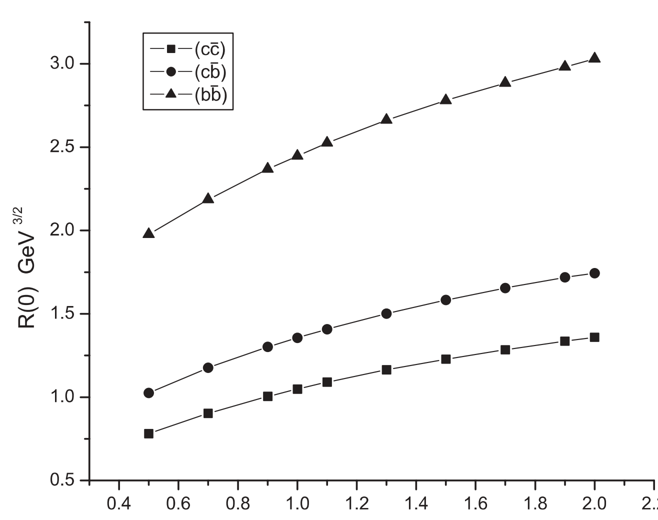

FIG. 2. $R(0) \rightarrow \nu$.

TABLE II. Wave function at the origin ($|R(0)|$) and spin average masses of the S-wave $c\bar{c}$ meson.

State	ν	$\bar{\mu}$ GeV	$\|R(0)\|$ GeV$^{3/2}$	$E(\bar{\mu})$ (GeV)	Exp. (GeV)	Theory (GeV)
$1S$	0.5	1.068	0.781	3.068		
	0.7	1.177	0.903	3.068		
	0.9	1.264	1.005	3.068		
	1.0	1.300	1.049	3.068		
	1.1	1.335	1.090	3.068	3.068	3.068[a]
	1.3	1.394	1.164	3.068		3.068[b]
	1.5	1.445	1.228	3.068		
	1.7	1.489	1.285	3.068		
	1.9	1.528	1.336	3.068		
	2.0	1.546	1.360	3.068		
$2S$	0.5	1.057	0.384	3.368		
	0.7	1.242	0.489	3.454		
	0.9	1.403	0.588	3.534		
	1.0	1.473	0.632	3.567		
	1.1	1.540	0.676	3.601	3.663	3.662[a]
	1.3	1.660	0.757	3.661		3.674[b]
	1.5	1.765	0.829	3.713		
	1.7	1.856	0.894	3.756		
	1.9	1.939	0.955	3.796		
	2.0	1.976	0.982	3.814		
$3S$	0.5	1.097	0.271	3.550		
	0.7	1.333	0.363	3.712		
	0.9	1.545	0.453	3.870		
	1.0	1.640	0.495	3.940		
	1.1	1.732	0.537	4.012	4.040	4.064[a]
	1.3	1.901	0.618	4.146		4.073[b]
	1.5	2.051	0.692	4.266		
	1.7	2.186	0.762	4.373		
	1.9	2.309	0.827	4.473		
	2.0	2.365	0.857	4.518		

[a]Reference [14].
[b]Reference [19].

TABLE III. Derivative of wave function at the origin ($|R'(0)|$) and P-wave masses of the $c\bar{c}$ meson.

State	ν	$\bar{\mu}$ GeV	$\|R'(0)\|$ GeV$^{5/2}$	$E(\bar{\mu})$ (GeV)	Exp. (GeV)	Theory (GeV)
$1P$	0.5	1.024	0.217	3.313		
	0.7	1.180	0.309	3.373		
	0.9	1.331	0.417	3.426		
	1.0	1.392	0.467	3.450		
	1.1	1.450	0.517	3.473	3.525	3.526[a]
	1.3	1.553	0.614	3.513		3.497[b]
	1.5	1.642	0.705	3.547		
	1.7	1.720	0.792	3.576		
	1.9	1.790	0.875	3.603		
	2.0	1.823	0.916	3.615		
$2P$	0.5	1.081	0.405	3.519		
	0.7	1.307	0.651	3.666		
	0.9	1.509	0.932	3.808		
	1.0	1.560	1.013	3.872		
	1.1	1.687	1.232	3.936		3.945[a]
	1.3	1.847	1.545	4.055		3.907[b]
	1.5	1.990	1.862	4.162		
	1.7	2.117	2.174	4.257		
	1.9	2.232	2.481	4.345		
	2.0	2.285	2.631	4.385		

[a]Reference [14].
[b]Reference [19].

a model-independent relationship similar to the one given by Ref. [42] as

$$|\psi_{b\bar{c}}|^2 \approx |\psi_{c\bar{c}}|^{2(1-q)}\,|\psi_{b\bar{b}}|^{2q} \tag{9}$$

with $q = 0.3$. This relation provides the $1S$ wave function at the origin within 2% variation for the choices of the potential range $0.5 \leqslant \nu \leqslant 2$. For $2S$ and $3S$ states we find the relation holds within 5% for all values for ν studied here. It is to be noted here that such a scaling law with smaller percentage variations exist here even though the potential contains a coulomb part.

A. Spin-hyperfine and spin-orbit splitting in heavy-heavy flavor mesons

In general, the quark-antiquark bound states are represented by $n^{2S+1}L_J$, identified with the J^{PC} values, with $\vec{J} = \vec{L} + \vec{S}$, $\vec{S} = \vec{S}_Q + \vec{S}_{\bar{Q}}$, parity $P = (-1)^{L+1}$, and the charge conjugation $C = (-1)^{L+S}$ and (n, L) are the radial quantum numbers. So the S-wave ($L = 0$) bound states are represented by $J^{PC} = 0^{-+}$ and 1^{--}, respectively. And the P-wave ($L = 1$) states are represented by $J^{PC} = 1^{+-}$ with $L = 1$ and $S = 0$, whereas $J^{PC} = 0^{++}$, 1^{++}, and 2^{++} correspond to $L = 1$ and $S = 1$, respectively. Accordingly, the spin-spin interaction among the constituent quarks provides the mass splitting of $J = 0^{-+}$ and 1^{--} states, whereas the spin-orbit interaction provides the mass splitting of $J^{PC} = 0^{++}, 1^{++}$, and 2^{++} states. The $J^{PC} = 1^{+-}$ state with $L = 1$ and $S = 0$ represents the center-of-weight mass of the P state as its spin-orbit contribution becomes zero, whereas the two $J = 1^{+-}$ singlet and the $J = 1^{++}$ of the triplet P states form a mixed sate. We add separately the spin-dependent part of the usual one-gluon-exchange potential (OGEP) between the quark-antiquark for computing the hyperfine and spin-orbit shifting of the low-lying S and P states. Accordingly, the spin-spin and spin-orbit interactions are taken as [43]

$$V_{S_Q \cdot S_{\bar{Q}}}(r) = \frac{8}{9}\frac{\alpha_s}{m_Q m_{\bar{Q}}}\vec{S}_Q \cdot \vec{S}_{\bar{Q}} 4\pi\delta(r) \tag{10}$$

$$V_{L\cdot S}(r) = \frac{4\,\alpha_s}{3\,m_Q m_{\bar{Q}}}\frac{\vec{L}\cdot\vec{S}}{r^3}. \tag{11}$$

The value of the radial wave function R(0) for 0^{-+} and 1^{--} states would be different due to their spin-dependent hyperfine interaction. The spin hyperfine interaction of the heavy flavor mesons are small and this can cause a small shift in the value of the wave function at the origin. Thus, many other models do not consider this contribution to their value of $R(0)$. However, we account this correction to the value of $R(0)$ by considering

$$R_{nJ}(0) = R(0)\left[1 + (\mathrm{SF})_J \frac{\langle \varepsilon_{SD}\rangle_{nJ}}{M_{\mathrm{SA}}}\right]. \tag{12}$$

TABLE IV. Wave function at the origin ($|R(0)|$) and spin average masses of the S-wave $b\bar{c}$ meson.

State	ν	$\bar{\mu}$ GeV	$\|R(0)\|$ GeV$^{3/2}$	$E(\bar{\mu})$ (GeV)	Theory (GeV)
1S	0.5	1.281	1.025	6.320	
	0.7	1.404	1.176	6.320	
	0.9	1.502	1.301	6.320	
	1.0	1.544	1.357	6.320	6.317[a]
	1.1	1.583	1.408	6.320	6.319[b]
	1.3	1.652	1.502	6.320	
	1.5	1.711	1.583	6.320	
	1.7	1.763	1.655	6.320	
	1.9	1.807	1.718	6.320	
	2.0	1.825	1.744	6.320	
2S	0.5	1.236	0.486	6.589	
	0.7	1.453	0.619	6.665	
	0.9	1.635	0.739	6.730	
	1.0	1.719	0.797	6.761	
	1.1	1.796	0.851	6.790	
	1.3	1.938	0.954	6.844	6.869[a]
	1.5	2.061	1.046	6.890	6.888[b]
	1.7	2.172	1.132	6.931	
	1.9	2.266	1.206	6.965	
	2.0	2.307	1.239	6.977	
3S	0.5	1.274	0.339	6.746	
	0.7	1.550	0.455	6.889	
	0.9	1.792	0.565	7.021	
	1.0	1.905	0.620	7.085	
	1.1	2.012	0.674	7.147	
	1.3	2.211	0.775	7.265	7.224[a]
	1.5	2.389	0.870	7.372	7.271[b]
	1.7	2.550	0.960	7.471	
	1.9	2.692	1.041	7.555	
	2.0	2.755	1.078	7.590	

[a]Reference [14].
[b]Reference [44].

Where $(\mathrm{SF})_J$ and $\langle\varepsilon_{SD}\rangle_{nJ}$ is the spin factor and spin interaction energy of the meson in the nJ state, whereas $R(0)$ and M_{SA} correspond to the radial wave function at the zero separation and spin average mass, respectively, of the $Q\bar{Q}$ system. It can be seen that Eq. (12) provides the average radial wave function given by Ref. [33] as

$$R(0) = \frac{R_p + 3R_v}{4}. \tag{13}$$

It is found that the computed mass increases with increase of ν. The computed results for the pseudoscalar (P) and vector (V) mesons in the case of $c\bar{c}$, $c\bar{b}$, and $b\bar{b}$ systems are tabulated in Tables VIII–X. The spin-spin hyperfine and spin-orbit interactions are computed perturbatively to get the masses of η_c, J/ψ, B_c, B_c^*, η_b, and Υ states. The results are compared with known experimental values as well as with other theoretical predictions. Mass predictions with ν between 1.0 and 1.5 are found in accordance with the experimental results [2].

TABLE V. Derivative of wave function at the origin ($|R'(0)|$) and the P-wave masses of $c\bar{b}$ mesons.

State	ν	$\bar{\mu}$ GeV	$\|R'(0)\|$ GeV$^{5/2}$	$E(\bar{\mu})$ (GeV)	Theory (GeV)
1P	0.5	1.198	0.321	6.542	
	0.7	1.392	0.467	6.597	
	0.9	1.553	0.613	6.641	
	1.0	1.625	0.687	6.662	
	1.1	1.692	0.760	6.682	
	1.3	1.814	0.905	6.718	6.749[a]
	1.5	2.920	1.042	6.749	6.736[b]
	1.7	2.013	1.173	6.777	
	1.9	2.094	1.296	6.799	
	2.0	2.129	1.349	6.806	
2P	0.5	1.260	0.594	6.720	
	0.7	1.520	0.950	6.851	
	0.9	1.751	1.353	6.969	
	1.0	1.859	1.571	7.027	
	1.1	1.961	1.794	7.082	
	1.3	2.149	2.257	7.188	7.145[a]
	1.5	2.317	2.725	7.283	7.142[b]
	1.7	2.469	3.184	7.370	
	1.9	2.603	3.644	7.445	
	2.0	2.662	3.852	7.476	

[a]Reference [14].
[b]Reference [44].

III. DECAY CONSTANTS ($f_{P/V}$) OF THE HEAVY FLAVORED MESONS

The decay constants of mesons are important parameters in the study of leptonic or nonleptonic weak decay processes. The decay constants of pseudoscalar (f_P) and vector (f_V) mesons are obtained by prarameterizing the matrix elements of weak current between the corresponding mesons and the vacuum as

$$\langle 0|\bar{Q}\gamma^\mu\gamma_5 Q|P_\mu(k)\rangle = i f_P k^\mu \tag{14}$$
$$\langle 0|\bar{Q}\gamma^\mu Q|V(k,\epsilon)\rangle = f_V M_V \epsilon^\mu, \tag{15}$$

where k is the meson momentum and ϵ^μ and M_V are the polarization vector and mass of the vector meson. In the relativistic quark model, the decay constant can be expressed through the meson wave function $\Phi_{P,V}(p)$ in the momentum space as [14]

$$f_{P,V} = \sqrt{\frac{12}{M_{P,V}}} \times \int \frac{d^3p}{(2\pi)^3}\sqrt{\left(\frac{E_Q(p)+m_Q}{2E_Q(p)}\right)}\sqrt{\left(\frac{E_{\bar{Q}}(p)+m_{\bar{Q}}}{2E_{\bar{Q}}(p)}\right)} \times \left\{1+\lambda_{P,V}\frac{p^2}{[E_Q(p)+m_Q][E_{\bar{Q}}(p)+m_{\bar{Q}}]}\right\}\Phi_{P,V}(p) \tag{16}$$

with $\lambda_P = -1$ and $\lambda_V = -1/3$. In the nonrelativistic limit $\frac{p^2}{m^2} \to 0$, this expression reduces to the well-known relation between $f_{P,V}$ and the ground-state wave function at the origin

TABLE VI. Wave function at the origin ($|R(0)|$) and the spin average masses of the S-wave $b\bar{b}$ meson.

State	ν	$\bar{\mu}$ GeV	$\lvert R(0)\rvert$ GeV$^{3/2}$	$E(\bar{\mu})$ (GeV)	Theory (GeV)
1S	0.5	1.985	1.977	9.453	
	0.7	2.122	2.186	9.453	
	0.9	2.238	2.368	9.453	
	1.0	2.288	2.447	9.453	
	1.1	2.336	2.525	9.453	9.445[a]
	1.3	2.402	2.662	9.453	9.453[b]
	1.5	2.491	2.780	9.453	
	1.7	2.554	2.885	9.453	
	1.9	2.611	2.982	9.453	
	2.0	2.638	3.030	9.453	
2S	0.5	1.701	0.784	9.701	
	0.7	1.979	0.984	9.758	
	0.9	2.227	1.175	9.812	
	1.0	2.338	1.264	9.838	
	1.1	2.442	1.349	9.861	10.016[a]
	1.3	2.636	1.513	9.905	10.008[b]
	1.5	2.807	1.663	9.944	
	1.7	2.958	1.790	9.977	
	1.9	3.094	1.924	10.008	
	2.0	3.158	1.984	10.023	
3S	0.5	1.692	0.519	9.826	
	0.7	2.053	0.694	9.935	
	0.9	2.385	0.868	10.043	
	1.0	2.538	0.953	10.095	
	1.1	2.684	1.036	10.144	10.348[a]
	1.3	2.957	1.199	10.241	10.351[b]
	1.5	3.205	1.353	10.330	
	1.7	3.427	1.496	10.410	
	1.9	3.631	1.631	10.485	
	2.0	3.727	1.696	10.522	

[a]Reference [14].
[b]Reference [45].

$\psi_{P,V}(0)$, the Van Royen-Weisskopf formula [46]. Though most of the models predict the mesonic mass spectrum successfully, there are disagreements in the predictions of the pseudoscalar and vector decay constants. For example, most of the cases, the ratio $\frac{f_P}{f_V}$ was predicted to be >1 as $m_P < m_V$ and their wave function at the origin $\psi_P(0) \sim \psi_V(0)$ [47]. The ratio computed in the relativistic models [47] predicted the ratio $\frac{f_P}{f_V} < 1$, particularly in the heavy flavors sector. The disparity of the predictions of these decay constants play decisive role in the precision measurements of the weak decay parameters. So we re-examine the predictions of the decay constants under different potential schemes discussed in the present work. Incorporating a first-order QCD correction factor, we compute them using the relation,

$$f_{P/V}^2 = \frac{12|\psi_{P/V}(0)|^2}{M_{P/V}}\bar{C}^2(\alpha_s), \tag{17}$$

where $\bar{C}(\alpha_s)$ is the QCD correction factor given by [48,49]

$$\bar{C}(\alpha_s) = 1 - \frac{\alpha_s}{\pi}\left(\delta^{P,V} - \frac{m_Q - m_{\bar{Q}}}{m_Q + m_{\bar{Q}}}\ln\frac{m_Q}{m_{\bar{Q}}}\right). \tag{18}$$

TABLE VII. Derivative of wave function at the origin ($|R'(0)|$) and the P-wave masses of the $b\bar{b}$ meson.

State	ν	$\bar{\mu}$ GeV	$\lvert R'(0)\rvert$ GeV$^{5/2}$	$E(\bar{\mu})$ (GeV)	Exp. (GeV)	Theory (GeV)
1P	0.5	1.654	0.718	9.670		
	0.7	1.904	1.021	9.712		
	0.9	2.121	1.337	9.751		
	1.0	2.218	1.446	9.768		
	1.1	2.308	1.653	9.784	9.900	9.901[a]
	1.3	2.474	1.966	9.815		9.900[b]
	1.5	2.621	2.271	9.842		
	1.7	2.750	2.559	9.864		
	1.9	2.866	2.838	9.885		
	2.0	2.921	2.977	9.896		
2P	0.5	1.669	1.200	9.808		
	0.7	2.016	1.922	9.908		
	0.9	2.333	2.770	10.006		
	1.0	2.478	3.223	10.053		
	1.1	2.617	3.692	10.097	10.260	10.261[a]
	1.3	2.876	4.677	10.184		10.258[b]
	1.5	3.111	5.691	10.264		
	1.7	3.321	6.699	10.335		
	1.9	3.513	7.708	10.401		
	2.0	3.604	8.218	10.434		

[a]Reference [14].
[b]Reference [45].

Here $\delta^P = 2$ and $\delta^V = 8/3$. The computed f_P and f_V for $c\bar{c}$, $c\bar{b}$, and $b\bar{b}$ systems using Eqs. (17) and (18) and the predicted radial wave functions at the origin $R_{nJ}(0)$ of the respective mesons are tabulated in Tables XI–XIII. The decay constants without and with the QCD corrections are also listed as $f_{P,V}$ and $f_{P,V}$(cor.) in the table. The plot of f_P vs. $(m_Q + m_{\bar{Q}})$ shows (see Fig. 3) deviations from linearity as against the predictions of a linear scaling between the weak decay constant and the sum of quark-antiquark masses justified within a renormalized light front QCD inspired model for quark antiquark bound states [50].

IV. WEAK DECAY OF B_c^+ MESON

The decay properties of $B_c^+(\bar{b}c)$ meson is of interest as it decays only through weak interactions [14,24,51,52]. This is due to the fact that its ground-state energy lies below the B D-threshold value of 7.15 GeV and has nonvanishing flavor. This eliminates the uncertainties encountered due to strong decays and provides a clear decay width and lifetime for B_c^+ meson, which helps to fix more precise value of the weak decay parameters such as the CKM mixing matrix elements (V_{cb}, V_{cs}) and the leptonic decay constant (f_P). Adopting the spectator model for the charm-beauty system [24], the total decay width of B_c^+ meson can be approximated as the sum of the widths of $\bar{b}$-quark decay keeping the c quark as spectator, the c-quark decay

TABLE VIII. S- and P-wave masses (in GeV) of the $c\bar{c}$ meson.

ν	1^1S_0	1^3S_1	1^1P_1	1^3P_0	1^3P_1	1^3P_2	2^1S_0	2^3S_1	2^1P_1	2^3P_0	2^3P_1	2^3P_2	3^1S_0	3^3S_1
0.5	3.000	3.092	3.313	3.292	3.302	3.323	3.352	3.375	3.519	3.494	3.507	3.531	3.541	3.553
0.7	2.980	3.100	3.373	3.341	3.357	3.389	3.427	3.464	3.666	3.623	3.644	3.687	3.697	3.717
0.9	2.960	3.109	3.429	3.383	3.406	3.451	3.495	3.547	3.808	3.742	3.775	3.842	3.846	3.878
1.0	2.950	3.112	3.450	3.398	3.424	3.477	3.522	3.583	3.872	3.792	3.832	3.911	3.912	3.950
1.1	2.942	3.116	3.473	3.414	3.444	3.503	3.549	3.619	3.936	3.843	3.889	3.983	3.979	4.024
1.3	2.926	3.123	3.513	3.441	3.477	3.550	3.597	3.683	4.055	3.933	3.994	4.116	4.102	4.161
1.5	2.912	3.129	3.547	3.461	3.504	3.590	3.636	3.739	4.162	4.009	4.085	4.239	4.212	4.285
1.7	2.899	3.134	3.576	3.477	3.526	3.625	3.668	3.788	4.257	4.073	4.165	4.394	4.309	4.395
1.9	2.887	3.141	3.603	3.491	3.547	3.658	3.696	3.832	4.345	4.129	4.237	4.453	4.396	4.500
2.0	2.882	3.144	3.615	3.497	3.556	3.673	3.708	3.852	4.385	4.153	4.269	4.501	4.436	4.547
[1,2]	2.980	3.097	3.511	3.415		3.556	3.622 [53]	3.686				3.929		4.040
[14]	2.979	3.096	3.526	3.424	3.511	3.556	3.588	3.686	3.945	3.854	3.929	3.972	3.991	4.088
[54]	2.980	3.097	3.527	3.416	3.508	3.558	3.597	3.686	3.960	3.844	3.894	3.994	4.014	4.095

TABLE IX. S- and P-wave masses (in GeV) of the $c\bar{b}$ meson.

ν	1^1S_0	1^3S_1	1^1P_1	1^3P_0	1^3P_1	1^3P_2	2^1S_0	2^3S_1	2^1P_1	2^3P_0	2^3P_1	2^3P_2	3^1S_0	3^3S_1
0.5	6.291	6.330	6.542	6.534	6.538	6.546	6.582	6.591	6.720	6.711	6.715	6.726	6.743	6.747
0.7	6.283	6.334	6.597	6.584	6.590	6.603	6.655	6.669	6.851	6.834	6.840	6.859	6.884	6.891
0.9	6.273	6.335	6.641	6.624	6.633	6.650	6.715	6.735	6.969	6.944	6.957	6.982	7.012	7.024
1.0	6.269	6.337	6.662	6.642	6.652	6.672	6.743	6.767	7.027	6.997	7.012	7.042	7.075	7.089
1.1	6.265	6.338	6.682	6.659	6.671	6.693	6.770	6.797	7.082	7.047	7.065	7.099	7.135	7.151
1.3	6.259	6.341	6.718	6.691	6.704	6.732	6.819	6.852	7.188	7.142	7.165	7.211	7.249	7.271
1.5	6.252	6.344	6.749	7.716	7.733	7.765	6.860	6.900	7.283	7.225	7.254	7.312	7.351	7.379
1.7	6.247	6.347	6.777	7.739	7.758	7.796	6.896	6.943	7.370	7.300	7.335	7.405	7.445	7.479
1.9	6.241	6.348	6.799	7.756	7.777	7.820	6.924	6.978	7.445	7.363	7.404	7.486	7.525	7.565
2.0	6.237	6.348	6.806	7.762	7.784	7.829	6.935	6.991	7.476	7.388	7.432	7.519	7.558	7.601
[14]	6.270	6.332	6.749	6.699	6.734	6.762	6.835	6.881	7.145	7.091	7.126	7.145	7.193	7.235
[44]	6.256	6.337	6.755	6.700	6.730	6.747	6.899	6.929	7.169	7.108	7.135	7.142	7.280	7.308

TABLE X. S- and P-wave masses (in GeV) of the $b\bar{b}$ meson.

ν	1^1S_0	1^3S_1	1^1P_1	1^3P_0	1^3P_1	1^3P_2	2^1S_0	2^3S_1	2^1P_1	2^3P_0	2^3P_1	2^3P_2	3^1S_0	3^3S_1
0.5	9.426	9.463	9.672	9.664	9.670	9.683	9.696	9.702	9.808	9.803	9.806	9.811	9.824	9.827
0.7	9.419	9.465	9.716	9.703	9.712	9.731	9.751	9.760	9.908	9.898	9.903	9.913	9.931	9.936
0.9	9.414	9.467	9.757	9.740	9.751	9.774	9.803	9.816	10.006	9.991	9.999	10.014	10.038	10.045
1.0	9.411	9.468	9.775	9.755	9.768	9.792	9.826	9.841	10.053	10.035	10.044	10.062	10.088	10.097
1.1	9.408	9.468	9.791	9.769	9.784	9.809	9.846	9.865	10.097	10.076	10.086	10.108	10.136	10.147
1.3	9.403	9.470	9.824	9.797	9.815	9.840	9.888	9.910	10.184	10.155	10.170	10.198	10.230	10.244
1.5	9.399	9.472	9.852	9.820	9.842	9.866	9.924	9.951	10.264	10.228	10.246	10.282	10.317	10.334
1.7	9.394	9.473	9.877	9.840	9.864	9.887	9.955	9.985	10.335	10.291	10.313	10.357	10.394	10.416
1.9	9.390	9.474	9.900	9.857	9.885	9.905	9.982	10.017	10.401	10.350	10.376	10.428	10.466	10.492
2.0	9.389	9.475	9.911	9.866	9.896	9.913	9.995	10.032	10.434	10.379	10.406	10.462	10.501	10.529
[1,2]		9.460		9.860	9.893	9.913		10.023		10.232	10.255	10.268		10.355
[14]	9.400	9.460	9.901	9.863	9.892	9.913	9.993	10.023	10.261	10.234	10.255	10.268	10.328	10.355
[54]	9.414	9.461	9.900	9.861	9.891	9.912	9.999	10.023	10.262	10.231	10.255	10.272	10.345	10.364

TABLE XI. Decay constants (f_P and f_V) (in MeV) of 1S and $c\bar{c}$ mesons states.

Models	$R_p(0)$ (GeV$^{3/2}$)	$R_v(0)$ (GeV$^{3/2}$)	f_P (MeV)	f_P(cor.) (MeV)	f_V (MeV)	f_V(cor.) (MeV)
ERHM	0.726	0.752	410	317	418	323
BT	0.874	0.909	499	382	505	389
PL	0.971	1.009	550	399	560	407
LOG	0.877	0.914	496	379	506	387
Cornell	1.171	1.217	663	532	676	543
$\nu = 0.5$	0.763	0.787	430	348	437	326
0.7	0.875	0.912	495	401	506	377
0.9	0.967	1.018	549	444	564	421
1.0	1.005	1.063	572	463	589	439
1.1	1.041	1.107	593	480	613	457
1.3	1.104	1.184	627	507	655	488
1.5	1.158	1.252	663	536	692	516
1.7	1.204	1.311	691	559	724	539
1.9	1.245	1.366	716	579	753	561
2.0	1.264	1.391	728	589	767	571
				335± 75 [55]	459± 28 [56]	416± 6 [55]

with the $\bar{b}$ quark as spectator, and the annihilation channel $B_c^+ \to l^+\nu_l(c\bar{s}, u\bar{s}), l = e, \mu, \tau$ with no interference assumed between them.

Accordingly, the total width is written as [24]

$$\Gamma(B_c \to X) = \Gamma(b \to X) + \Gamma(c \to X) + \Gamma(\text{Anni}). \quad (19)$$

Neglecting the quark binding effects, we obtain for the b and c inclusive widths in the spectator approximation as [24]

$$\begin{aligned}\Gamma(b \to X) &= \frac{9\, G_F^2\, |V_{cb}|^2\, m_b^5}{192\,\pi^3}\\ &= 7.97 \times 10^{-4}\ \text{eV (a)}\\ &= 8.66 \times 10^{-4}\ \text{eV (b)} \qquad (20)\\ \Gamma(c \to X) &= \frac{5\, G_F^2\, |V_{cs}|^2\, m_c^5}{192\,\pi^3}\\ &= 4.13 \times 10^{-4}\ \text{eV(a)}\\ &= 4.15 \times 10^{-4}\ \text{eV(b)} \qquad (21)\end{aligned}$$

TABLE XII. Pseudoscalar and vector-meson decay constants (f_P and f_V) (in MeV) of 1S $b\bar{c}$ meson state.

	$R_p(0)$	$R_v(0)$	f_P	f_P(cor.)	f_V	f_V(cor.)
$\nu = 0.5$	1.021	1.027	398	356	399	336
0.7	1.169	1.178	456	408	457	385
0.9	1.291	1.304	504	451	506	426
1.0	1.346	1.361	525	470	528	445
1.1	1.396	1.413	545	488	548	461
1.3	1.487	1.507	581	520	585	492
1.5	1.565	1.589	612	548	616	519
1.7	1.635	1.662	639	572	645	542
1.9	1.695	1.725	663	594	669	563
2.0	1.722	1.758	674	603	682	574
				433 [14]	503 [14]	418 ± 24 [56]

TABLE XIII. Decay constants (f_P and f_V) (in MeV) of 1S $b\bar{b}$ meson state.

Models	$R_p(0)$ (GeV$^{3/2}$)	$R_v(0)$ (GeV$^{3/2}$)	f_P (MeV)	f_P(cor.) (MeV)	f_V (MeV)	f_V(cor.) (MeV)
ERHM	2.232	2.235	709	601	710	601
BT	2.527	2.551	807	683	810	686
PL	2.132	2.146	680	563	682	565
LOG	2.206	2.221	703	594	706	596
Cornell	3.706	3.762	1185	1022	1194	1029
$\nu = 0.5$	1.971	1.979	627	537	629	509
0.7	2.178	2.189	693	594	695	563
0.9	2.358	2.371	751	643	753	609
1.0	2.436	2.451	776	665	778	630
1.1	2.513	2.529	801	686	803	650
1.3	2.648	2.667	844	723	847	685
1.5	2.764	2.785	881	755	884	715
1.7	2.867	2.891	914	783	918	743
1.9	2.962	2.989	945	809	949	768
2.0	3.009	3.037	960	822	964	780
				711 [19]		708 ± 8 [37]

Here we have used the model quark masses and the two values (a) and (b) correspond to the two set of values for the CKM matrix elements (a)→ $|V_{cs}| = 0.97296, |V_{cb}| = 0.04221$ as used in Ref. [1] and (b)→ $|V_{cs}| = 0.975, |V_{cb}| = 0.044$ as the upper bound provided by the Particle Data Group. The values of $\Gamma(B \to X)$ and $\Gamma(c \to X)$ in Bethe-Salpeter model [24] and relativized quark model [51] are 7.5 and 5.1 and then 4.8 and 3.3 (widths are in 10^{-4} eV), respectively.

Employing the computed mass of the 1^1S_0 state (M_{B_c}) and f_{B_c} values obtained from the present study, the width of the annihilation channel is computed using the expression given by [24],

$$\Gamma(\text{Anni}) = \frac{G_F^2}{8\pi}\, |V_{bc}|^2\, f_{B_C}^2 M_{bc} m_i^2 \left(1 - \frac{m_q^2}{M_{B_c}^2}\right)^2 C_q, \quad (22)$$

where $C_q = 3|V_{cs}|^2$ for $c\bar{s}$ and m_q is the mass of the heaviest fermions.

The computed widths and lifetime in our CPP$_\nu$ model are listed in Table XIV. Our predictions for the lifetime with the potential index $0.5 \succeq \nu \succeq 2$ lies well within the experimental error bar.

V. DECAY RATES OF QUARKONIA

Along with the mass spectrum, successful predictions of various decay widths of heavy flavored systems have remained as a testing ground for the success of phenomenological models. Experimentally, the excited states and the leptonic, di-γ, and other hadronic decay widths of the heavy flavor mesons have been reported. However, experimentally, the pseudoscalar $b\bar{b}$ bound state η_b is still elusive though experimental search for this state at the di-γ decay channel has been initiated recently [47].

TABLE XIV. Decay widths (in 10^{-4} eV) and lifetime τ (in ps) of B_c^+ meson.

Model	Γ(Anni)		$\Gamma(B_c \to X)$		τ (in PS)	
	a	*b*	*a*	*b*	*a*	*b*
$\nu = 0.5$	0.370	0.370	12.47	13.18	0.530	0.499
0.7	0.486	0.484	12.59	13.30	0.523	0.495
0.9	0.596	0.593	12.70	13.41	0.518	0.491
1.0	0.644	0.642	12.75	13.46	0.516	0.489
1.1	0.693	0.690	12.79	13.51	0.515	0.487
1.3	0.786	0.783	12.89	13.60	0.511	0.484
1.5	0.871	0.867	12.89	13.68	0.507	0.481
1.7	0.951	0.950	12.97	13.76	0.504	0.478
1.9	1.023	1.020	13.05	13.83	0.502	0.476
2.0	1.053	1.050	13.15	13.87	0.500	0.475
[1]					$0.46^{+0.18}_{-0.16}$	
[24]		1.40		14.00	0.47	
[51]		0.67		8.8	0.75	

As an attempt to improve the theoretical predictions involving the phenomenological description of the meson, using the radial wave functions and other model parameters of the different potential models we study the decay of $^1S_0$ quarkonium into di-γ and the decay of $^3S_1$ into lepton pairs using the NRQCD formalism [33]. It is expected that the

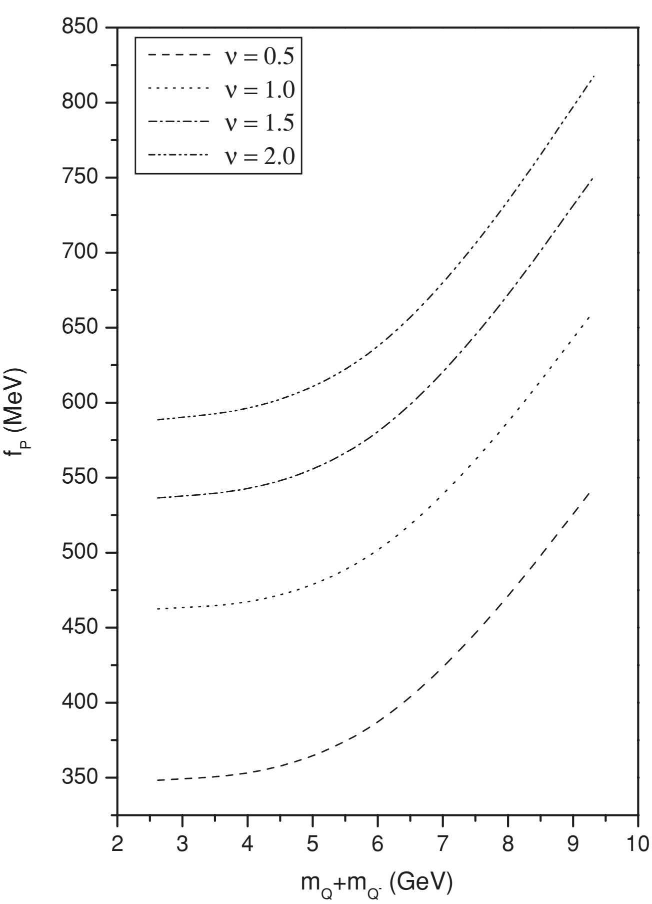

FIG. 3. Trend line for f_p with $m_Q + m_{\bar{Q}}$.

NRQCD formalism has all the corrective contributions for the right predictions of the decay rates. NRQCD factorization expressions for the decay rates of quarkonium and decay are given by [31]

$$\begin{aligned}\Gamma(^1S_0 \to \gamma\gamma) &= \frac{F_{\gamma\gamma}(^1S_0)}{m_Q^2}|\langle 0|\chi^\dagger\psi|^1S_0\rangle|^2 + \frac{G_{\gamma\gamma}(^1S_0)}{m_Q^4}\\ &\times Re\left[\langle ^1S_0|\psi^\dagger\chi|0\rangle\langle 0|\chi^\dagger\left(-\frac{i}{2}\vec{D}\right)^2\psi|^1S_0\rangle\right]\\ &+\frac{H^1_{\gamma\gamma}(^1S_0)}{m_Q^6}\langle ^1S_0|\psi^\dagger\left(-\frac{i}{2}\vec{D}\right)^2\chi|0\rangle\\ &\times\langle 0|\chi^\dagger\left(-\frac{i}{2}\vec{D}\right)^2\psi|^1S_0\rangle\\ &+\frac{H^2_{\gamma\gamma}(^1S_0)}{m_Q^6}Re\left[\langle ^1S_0|\psi^\dagger\chi|0\rangle\langle 0|\chi^\dagger\left(-\frac{i}{2}\vec{D}\right)^4\psi|^1S_0\rangle\right]\end{aligned} \quad (23)$$

$$\begin{aligned}\Gamma(^3S_1 \to e^+e^-) &= \frac{F_{ee}(^3S_1)}{m_Q^2}|\langle 0|\chi^\dagger\sigma\psi|^3S_1\rangle|^2 + \frac{G_{ee}(^3S_1)}{m_Q^4}\\ &\times Re\left[\langle ^3S_1|\psi^\dagger\sigma\chi|0\rangle\langle 0|\chi^\dagger\sigma\left(-\frac{i}{2}\vec{D}\right)^2\psi|^3S_1\rangle\right]\\ &+\frac{H^1_{ee}(^1S_0)}{m_Q^6}\langle ^3S_1|\psi^\dagger\sigma\left(-\frac{i}{2}\vec{D}\right)^2\chi|0\rangle\\ &\times\langle 0|\chi^\dagger\sigma\left(-\frac{i}{2}\vec{D}\right)^2\psi|^3S_1\rangle + \frac{H^2_{ee}(^1S_0)}{m_Q^6}\\ &\times Re\left[\langle ^3S_1|\psi^\dagger\sigma\chi|0\rangle\langle 0|\chi^\dagger\sigma\left(-\frac{i}{2}\vec{D}\right)^4\psi|^3S_1\rangle\right].\end{aligned} \quad (24)$$

The short-distance coefficients (F and G) of the order of α_s^2 and α_s^3 are given by [31]

$$F_{\gamma\gamma}(^1S_0) = 2\pi Q^4\alpha^2\left[1+\left(\frac{\pi^2}{4}-5\right)C_F\frac{\alpha_s}{\pi}\right] \quad (25)$$

$$G_{\gamma\gamma}(^1S_0) = -\frac{8\pi Q^4}{3}\alpha^2 \quad (26)$$

$$H^1_{\gamma\gamma}(^1S_0) + H^2_{\gamma\gamma}(^1S_0) = \frac{136\pi}{45}Q^4\alpha^2 \quad (27)$$

$$\begin{aligned}F_{ee}(^3S_1) &= \frac{2\pi Q^2\alpha^2}{3}\left\{1-4C_F\frac{\alpha_s(m)}{\pi}\right.\\ &+\left[-117.46+0.82n_f\right.\\ &\left.\left.+\frac{140\pi^2}{27}ln\left(\frac{2m}{\mu_A}\right)\right]\left(\frac{\alpha_s}{\pi}\right)^2\right\}\end{aligned} \quad (28)$$

$$G_{ee}(^3S_1) = -\frac{8\pi Q^2}{9}\alpha^2 \quad (29)$$

TABLE XV. Decay rates (in keV) of $0^{-+} \to \gamma\gamma$ and the relevant correction terms of η_c and η_b mesons.

Systems	Models	Γ_0	Γ_R	Γ	$\Gamma_{\rm NRQCD}$ Up to $O(v^0)$	$\Gamma_{\rm NRQCD}$ Up to $O(v^4)$	$\Gamma_{\rm NRQCD_{frs}}$	$\Gamma_{\rm Others}$
	ERHM	7.460	−2.855	4.605	4.005	4.225	–	
	BT	10.870	−4.206	6.664	6.555	6.561	–	7.2 ± 0.7 ± 2.0 [1]
	PL(Martin)	13.406	−6.196	7.210	8.434	10.691	–	7.500 [57]
η_c	Log	10.937	−4.349	6.588	6.691	6.697	–	
	Cornell	19.512	−6.581	12.931	13.779	17.447	–	9.02 ± 0.79 [58]
	CPP$_\nu$ = 0.5	8.173	−2.635	5.538	2.511	6.078	2.992	
	0.7	10.918	−3.521	7.397	3.706	7.810	4.087	
	0.9	13.465	−4.342	9.123	4.925	9.391	5.102	
	1.0	14.649	−4.724	9.925	5.552	10.077	5.549	
	1.1	15.812	−5.099	10.713	6.171	10.761	6.012	
	1.3	17.987	−5.800	12.187	7.387	12.016	7.095	
	1.5	19.971	−6.440	13.531	8.556	13.142	7.536	
	1.7	22.788	−7.026	15.762	9.700	14.166	8.170	
	1.9	23.502	−7.578	16.924	10.789	15.139	8.736	
	2.0	24.297	−7.835	16.462	11.295	15.596	9.006	
	ERHM	0.444	−0.114	0.326	0.315	0.317	–	
	BT	0.574	−0.149	0.424	0.445	0.455	–	
	PL (Martin)	0.406	−0.118	0.288	0.312	0.340	–	0.364 [33]
η_b	Log	0.435	−0.115	0.320	0.337	0.345	–	0.490 [57]
	Cornell	1.244	−0.290	0.954	1.015	1.112	–	
	CPP$_\nu$ = 0.5	0.345	−0.086	0.259	0.254	0.254	0.195	
	0.7	0.422	−0.106	0.316	0.310	0.311	0.256	
	0.9	0.495	−0.124	0.371	0.365	0.366	0.321	
	1.0	0.529	−0.132	0.397	0.390	0.391	0.353	
	1.1	0.563	−0.141	0.422	0.416	0.416	0.386	
	1.3	0.626	−0.156	0.470	0.462	0.463	0.435	
	1.5	0.683	−0.171	0.512	0.505	0.505	0.510	
	1.7	0.735	−0.184	0.551	0.544	0.545	0.570	
	1.9	0.786	−0.196	0.590	0.582	0.582	0.628	
	2.0	0.811	−0.203	0.608	0.600	0.601	0.657	

ERHM [19,20], BT [5], PL (Martin) [6], Log [9], Cornell [11]

$$H^1_{ee}(^3S_1) + H^2_{ee}(^3S_1) = \frac{58\pi}{54}Q^2\alpha^2. \tag{30}$$

The matrix elements that contributes to the decay rates of the S-wave states into $\eta_Q \to \gamma\gamma$ and $\psi \to e^+e^-$ through next-to-leading order in v^2, the vacuum-saturation approximation gives [33]

$$\langle ^1S_0|\mathcal{O}(^1S_0)|^1S_0\rangle = |\langle 0|\chi^\dagger\psi|^1S_0\rangle|^2[1+O(v^4\Gamma)] \tag{31}$$

$$\langle ^3S_1|\mathcal{O}(^3S_1)|^3S_1\rangle = |\langle 0|\chi^\dagger\sigma\psi|^3S_1\rangle|^2[1+O(v^4\Gamma)] \tag{32}$$

$$\langle ^1S_0|\mathcal{P}_1(^1S_0)|^1S_0\rangle = Re\left[\langle ^1S_0|\psi^\dagger\chi|0\rangle\langle 0|\chi^\dagger\left(-\frac{i}{2}\vec{D}\right)^2 \times\psi|^1S_0\rangle\right] + O(v^4\Gamma) \tag{33}$$

$$\langle ^3S_1|\mathcal{P}_1(^3S_1)|^3S_1\rangle = Re\left[\langle ^3S_1|\psi^\dagger\sigma\chi|0\rangle\langle 0|\chi^\dagger \times\sigma\left(-\frac{i}{2}\vec{D}\right)^2\psi|^3S_1\rangle\right] + O(v^4\Gamma) \tag{34}$$

$$\langle ^1S_0|\mathcal{Q}^1_1(^1S_0)|^1S_0\rangle = \langle 0|\chi^\dagger\left(-\frac{i}{2}\vec{D}\right)^2\psi|^1S_0\rangle \tag{35}$$

$$\langle ^3S_1|\mathcal{Q}^1_1(^3S_1)|^3S_1\rangle = \langle 0|\chi^\dagger\sigma\left(-\frac{i}{2}\vec{D}\right)^2\psi|^3S_1\rangle \tag{36}$$

$$\langle ^1S_0|\mathcal{Q}^2_1(^1S_0)|^1S_0\rangle = \langle 0|\chi^\dagger\left(-\frac{i}{2}\vec{D}\right)^4\psi|^1S_0\rangle \tag{37}$$

$$\langle ^3S_1\big|\mathcal{Q}^2_1(^3S_1)\big|^3S_1\rangle = \langle 0|\chi^\dagger\sigma\left(-\frac{i}{2}\vec{D}\right)^4\psi|^3S_1\rangle \tag{38}$$

The vacuum saturation allows the matrix elements of some four fermion operators to be expressed in terms of the regularized wave-function parameters given by [33]

$$\langle ^1S_0|\mathcal{O}(^1S_0)|^1S_0\rangle = \frac{3}{2\pi}|R_P(0)|^2 \tag{39}$$

$$\langle ^3S_1|\mathcal{O}(^3S_1)|^3S_1\rangle = \frac{3}{2\pi}|R_V(0)|^2 \tag{40}$$

$$\langle ^1S_0|\mathcal{P}_1(^1S_0)|^1S_0\rangle = -\frac{3}{2\pi}|\overline{R_P^*}\,\overline{\nabla^2R_P}| \tag{41}$$

TABLE XVI. Decay rates (in keV) of $1^{--} \to l^+l^-$ and the relevant correction terms of J/ψ and Υ mesons.

Systems	Models	Γ_{VW}	Γ_{rad}	Γ	Γ_{NRQCD}		$\Gamma_{\mathrm{NRQCD}_{\mathrm{frs}}}$	Γ_{EXP} [1]
					Up to $O(v^0)$	Up to $O(v^4)$		
	ERHM	5.595	−3.381	2.214	2.543	3.246	–	
J/ψ	BT	8.152	−4.982	3.170	2.539	2.809	–	5.55 ± 0.14 ± 0.02
	PL (Martin)	10.055	−7.341	2.714	3.311	4.698	–	
	Log	8.203	−0.171	3.057	1.967	2.094	–	
	Cornell	14.634	−7.701	6.933	7.920	10.294	–	
	$\mathrm{CPP}_\nu = 0.5$	6.130	−0.624	5.506	4.212	4.973	0.973	
	0.7	8.189	−0.845	7.344	6.199	7.701	1.676	
	0.9	10.153	−1.065	9.088	8.320	10.815	2.447	
	1.0	11.053	−1.165	9.888	9.353	12.398	2.822	
	1.1	11.946	−1.268	10.678	10.430	14.089	3.227	
	1.3	13.621	−1.463	12.158	12.558	17.550	3.996	
	1.5	15.165	−1.645	13.520	12.605	19.037	4.749	
	1.7	16.582	−1.813	14.769	16.643	24.587	5.467	
	1.9	17.920	−1.982	15.938	18.659	28.232	6.185	
	2.0	18.549	−2.061	16.488	19.634	30.032	6.534	
	ERHM	1.320	−0.540	1.303	1.221	1.228	–	
Υ	B.T.	1.720	−0.076	1.644	1.249	1.267	–	
	PL (Martin)	1.218	−0.761	0.457	0.693	0.774	–	1.340
	Log	1.305	−0.032	1.273	0.924	0.943	–	± 0.018
	Cornell	3.733	−0.232	3.501	2.025	2.270	–	
	$\mathrm{CPP}_\nu = 0.5$	1.035	−0.010	1.025	0.935	0.938	0.710	1.43 [59]
	0.7	1.266	−0.013	1.253	1.144	1.148	0.933	
	0.9	1.485	−0.015	1.470	1.344	1.349	1.165	
	1.0	1.587	−0.017	1.570	1.436	1.442	1.279	
	1.1	1.690	−0.018	1.678	1.529	1.535	1.397	
	1.3	1.878	−0.020	1.858	1.702	1.709	1.575	
	1.5	2.047	−0.022	2.025	1.857	1.865	1.844	
	1.7	2.206	−0.024	2.182	2.002	2.010	2.057	
	1.9	2.357	−0.026	2.331	2.141	2.149	2.266	
	2.0	2.433	−0.026	2.407	2.210	2.219	2.371	

ERHM [19,20], BT [5], PL (Martin) [6], Log [9], Cornell [11]

$$\langle {}^3S_1|\mathcal{P}_1({}^3S_1)|{}^3S_1\rangle = -\frac{3}{2\pi}|\overline{R_V^*}\overline{\nabla^2 R_V}| \tag{42}$$

$$\left\langle {}^1S_0\middle|\mathcal{Q}_1^1({}^1S_0)\middle|{}^1S_0\right\rangle = -\sqrt{\frac{3}{2\pi}}\overline{\nabla^2}R_P \tag{43}$$

$$\left\langle {}^3S_1\middle|\mathcal{Q}_1^1({}^3S_1)\middle|{}^3S_1\right\rangle = -\sqrt{\frac{3}{2\pi}}\overline{\nabla^2}R_V \tag{44}$$

$$\left\langle {}^1S_0\middle|\mathcal{Q}_1^2({}^1S_0)\middle|{}^1S_0\right\rangle = \frac{3}{2\pi}\nabla^2(\overline{\nabla^2}R_P) \tag{45}$$

$$\left\langle {}^3S_1\middle|\mathcal{Q}_1^2({}^3S_1)\middle|{}^3S_1\right\rangle = \frac{3}{2\pi}\nabla^2(\overline{\nabla^2}R_V). \tag{46}$$

We have computed the $\overline{\nabla}^2 R_{p/v}$ term as per Ref. [60]. Accordingly,

$$\nabla^2 R = -\epsilon_B R\frac{M}{2}, \quad \text{as} \quad r \to 0, \tag{47}$$

where ϵ_B is the binding energy and M is the mass of the respective mesonic state. The binding energy is computed as $\epsilon_B = M - (2m_Q)$. The right-hand side of Eqs. (45) and (46) are computed by assuming that $\langle p^2\rangle^2 \approx \langle p^4\rangle$. For comparison, we also compute the decay widths with the conventional Van Royen-Weisskopf (VW) formula with and without the radiative corrections.

Accordingly, the two photon decay width of the pseudoscalar meson is given by [22]

$$\Gamma(0^{-+}\to 2\gamma) = \Gamma_0 + \Gamma_R. \tag{48}$$

Here Γ_0 is the conventional Van Royen-Weisskopf term for the $0^{-+} \to \gamma\gamma$ decays [46], where Γ_R is due to the radiative corrections for this decay which is given by

$$\Gamma_0 = \frac{12\alpha_e^2 e_Q^4}{M_P^2}R_P^2(0) \tag{49}$$

and

$$\Gamma_R = \frac{\alpha_s}{\pi}\left(\frac{\pi^2 - 20}{3}\right)\Gamma_0. \tag{50}$$

Similarly, the leptonic decay width of the vector meson is computed as

$$\Gamma(1^{--} \to l^+l^-) = \Gamma_{\mathrm{VW}} + \Gamma_{\mathrm{rad}}, \tag{51}$$

where

$$\Gamma_{\text{VW}} = \frac{4\alpha_e^2 e_Q^2}{M_V^2} R_V^2(0). \tag{52}$$

Γ_{rad}, the radiative correction, is given by

$$\Gamma_{\text{rad}} = \frac{-16}{3\pi}\alpha_s \Gamma_{\text{VW}}. \tag{53}$$

It is obvious to note that the computations of the decay rates and the radiative correction term described here require the right description of the meson state through its radial wave function at the origin, $R(0)$, and its mass, M, along with other model parameters like α_s and the model quark masses. Generally, due to lack of exact solutions for color dynamics, $R_{P/V}(0)$ and M are considered free parameters of the theory [60]. However, it is appropriate to employ the phenomenological model spectroscopic parameters such as of the predicted mesonic mass and the corresponding wave function for the computations of the decay widths. In many cases of potential model predictions, the radial wave function at the origin are overestimated as far as the decay rates are concerned. In such cases, it is argued that the decay of $Q\bar{Q}$ occurs not at zero separation but at some finite $Q\bar{Q}$ radial separation. Then arbitrary scaling of the radial wave function at zero separation is done to estimate the decay rates correctly [11]. In the present computation of the decay rates using the NRQCD formalism we present our results obtained by using the radial wave function and their derivatives at zero separation (Γ_{NRQCD}) as well as at a finite radial separation of r_o, ($\Gamma_{\text{NRQCD}_{\text{frs}}}$). We defined r_o by

$$r_o = \frac{N_c |e_Q|}{M_{P/V}} \tag{54}$$

of the mesonic state. It is similar to the compton radius and we call it the color compton radius of the $Q\bar{Q}$ systems. Here, $N_c = 3$ and e_Q are the charge of the quark in terms of the electron charge.

The computed decay widths for $0^{-+} \to \gamma\,\gamma$ are presented in Table XV and for $1^{--} \to l^+l^-$ are listed in Table XVI. In the case of Γ_{NRQCD} terms up to $O(v^2)$ and terms up to $O(v^4)$ are separately tabulated to highlight their contributions in the respective decays.

VI. CONCLUSION AND DISCUSSION

In this article, we have made a comprehensive study of the heavy-heavy flavor mesonic systems in the general framework of potential models. The potential model parameters and the masses of the charmed and beauty quark obtained from the respective quarkonia mass predictions have been employed to study their decay properties in the framework of the NRQCD formalism as well as using the conventional Van Royen-Weisskopf nonrelativistic formula. We have also made a parameter-free prediction of the weak decay properties of B_c meson. The weak decay constants of the pseudoscalar (f_P) and the vector meson (f_V) computed here are is found to be in accordance with the recent predictions based on the relativistic Bethe-Salpeter method [56]. The departure from the predicted linear dependence of f_P with the mesonic masses within the effective light-front model in the heavy flavor sector suggest the requirement of more refined mechanism related to their wave functions incorporating the confinement and hyperfine splitting.

Masses of the pseudoscalar and vector mesons and the values of the radial wave function at the origin for $c\bar{c}$, $c\bar{b}$, and $b\bar{b}$ systems are computed in different potential schemes. The respective decay constants (f_P, f_V) are computed with and without QCD corrections. Using the predicted masses and radial wave functions at the origin, the di-γ, leptonic, light hadronic decays of quarkonia and the weak decay properties of B_c^+ mesons are studied. For the mass predictions and for the decay rates the present results based on (CPP_ν) are found to be in accordance with other potential model predictions as well as with the experimental values.

The theoretical (CPP_ν) predictions of the decay widths for $J/\psi \to l^+l^-$ and $\Upsilon \to l^+l^-$ as presented in Table XVI are found to be in accordance with other potential model predictions with the radiative correction as well as with the widths computed using NRQCD formalism.

Though the radiative corrections are found to be important in most of the phenomenological models, the NRQCD predictions with their matrix elements computed at finite radial separation defined through the "color compton radius" are found to be in better agreement with the experimental values for most of the cases.

It is interesting to note that the ERHM [20] predictions of the di-γ decay widths of η_c and leptonic decay widths of J/ψ and Υ are in good agreement with the respective experimental results with out any correction to the Van Royen-Weisskopf formula.

The NRQCD width for $\eta_c \to \gamma\gamma$ predicted in the present study based on the potential model parameters of BT [5], Log [9], and $\text{CPP}_\nu = 0.7, 0.9$ are close to the experimental value of $7.2 \pm 0.7 \pm 2.0$ keV reported by PDG2006 [1]. However, for the $\eta_b \to \gamma\gamma$ case, most of the model predictions based on the NRQCD formalism are very close to similar theoretical predictions of Ref. [33]. The predictions based on the V-W formula with radiative corrections are also found to be in close agreement with the prediction of Refs. [33] and [57], respectively.

The predictions of η_b mass spectra, its hyperfine mass split ($\Upsilon - \eta_b$) of 60 MeV, its decay constant f_P, and the di-γ width, etc., are important for the experimental hunting of η_b state. In the case of the dileptonic width of $c\bar{c}$ state, our predictions based on the NRQCD formalism with the finite-range correction for the interquark potential index $1.5 \leqslant \nu \leqslant 1.7$ are in fair agreement with the experimental value of 5.55 ± 0.14 keV, whereas for the $b\bar{b}$ system the $\text{NRQCD}_{\text{frs}}$ prediction is in good agrement with value of 1.340 ± 0.018 keV for the potential index $\nu = 1.1$. The $\text{CPP}_{\nu=0.5}$ predictions based on V-W with radiative correction is also found to be in good agreement with the expected values while in all other choices of ν over estimates the decay width. It indicates the importance of the computation from of the decay width at finite range of quark-antiquark separation.

In the case of the leptonic decay width of $\Upsilon(1S)$ state, most of the models do provide the decay widths in close agreement with the expected value either using NRQCD formalism or using V-W with radiative corrections. Here, again the ERHM prediction for both J/ψ and Υ are found to be very close to the respective experimental values with the conventional V-W formula only. It is suggests the adequacy of the model parameters that provide the spectroscopy as well as the decay properties.

To summarize, we find that the spectroscopy of $c\bar{c}$ system ($1S$ to $3S$) studied here are in good agreement with the respective experimental values in the potential range of $1.1 \leqslant \nu \leqslant 1.3$. However, the spectroscopic predictions with potential index $\nu = 1.5$ for $b\bar{b}$ system are found to be in agreement with the respective experimental values. The spectroscopic predictions of the $b\bar{c}$ system in the potential range $1.1 \leqslant \nu \leqslant 1.3$ are found to be in accordance with other model predictions.

In the case of the di-γ decay widths of the $c\bar{c}$ system, better agreement occurs for the potential index $\nu = 0.7$ under the NRQCD and the conventional V-W formula with radiative correction. However, the $\mathrm{NRQCD_{frs}}$ provides the experimental value of the decay width in the potential index range of $1.3 \leqslant \nu \leqslant 1.5$ only. For the $b\bar{b}$ system, better consistency in the predictions of both the leptonic and di-γ widths are observed around the potential index $0.7 \leqslant \nu \leqslant 1.1$.

The present study of the decay rates of quarkonia clearly indicates the relative importance of QCD-related corrections on the phenomenological potential models. The success of potential models in the determination of the S- and P-wave masses and decay rates of $c\bar{c}$, $b\bar{c}$, and $b\bar{b}$ systems are areas of future research, especially with regard to studying various transition rates and excited states of these mesonic systems. With the masses and wave functions of the heavy flavor mesons at hand, it would be rather simple to compute various transition rates such as $E1$ and $M1$ in these mesons. Such computations largely form the future applications of the present study. The decay rates and branching ratios of heavy flavor mesonic bound states are important ingredients in our present understanding of QCD.

The semileptonic decays offer an extremely favorable testing ground for perturbative QCD, radiative corrections, and nonperturbative QCD effects such as decay constants, form factors, and the best possible estimations of the CKM matrix elements. With the mass parameters of the beauty and the charm quark fixed from the study of its spectra, we have successfully computed the semileptonic decay width of the B_c meson.

The partial widths obtained here within the spectator model are compared with those obtained though the Bethe-Salpeter approach [24] as well as that from a relativistic quark model [51] in Table XIV. We obtained a higher branching ratio in the b-decay channel compared to other approaches as seen from in Table XIV. We get about 64% as the branching fractions of b-quark decay, about 33% as that of c-quark decay, and about 3% in the annihilation channel. However, the CKM mixing matrix elements V_{cb} and V_{cs} used as free parameters in all the three models are different but lie within the range given in the Particle Data Group [2]. The lifetime of B_c^+ predicted by the present calculation is found to be in good agreement with the experimental values as well as that by the Bethe-Salpeter method [24]. The predicted values from the relativistic model [51] is found to be far from the experimental values as well as other theoretical models.

Another aspect of the present study is that the decay of $Q\bar{Q}$ system occurs at a finite range of its separation provided by the color compton radius. This enable us to understand at least qualitatively the importance of various processes that occur at different radial seperation.

In conclusion, we have studied the importance of the spectroscopic parameters of different potential models in the predictions of the low-lying states of $c\bar{c}$, $c\bar{b}$, and $b\bar{b}$ systems as well as their decay properties in the frame work of the NRQCD formalism.

ACKNOWLEDGMENTS

The work is partially supported by Department of Science and Technology, Government of India, under a major research project, SR/S2/HEP-20/2006. Ajay Kumar Rai thanks Namit Mahajan of the Physical Research Laboratory, Ahmedabad, for useful discussions and suggestions.

[1] W.-M. Yao *et al.* (Particle Data Group), J. Phys. G **33**, 1 (2006).
[2] K. Hagiwara *et al.* (Particle Data Group), Phys. Rev. D **66**, 010001 (2002).
[3] M. B. Voloshin, Prog. Part. Nucl. Phys. **61**, 455 (2008).
[4] E. Eichten, S. Godfrey, Hanna Mahlke, and J. L. Rosner, Rev. Mod. Phys. **80**, 1161 (2008).
[5] Buchmuller and Tye, Phys. Rev. D **24**, 132 (1981).
[6] A. Martin, Phys. Lett. **B93**, 338 (1980).
[7] A. Martin, Phys. Lett. **B82**, 272 (1979).
[8] J. L. Richardson, Phys. Lett. **B82**, 272 (1979).
[9] C. Quigg and J. L. Rosner, Phys. Lett. **B71**, 153 (1977).
[10] C. Quigg and J. L. Rosner, Phys. Rep. **56**, 167 (1979).
[11] E. Eichten, K. Gottfried, T. Kinoshita, K. D. Lane, and T. M. Yan, Phys. Rev. D **17**, 3090 (1978).
[12] K. B. Vijaya Kumar, B. Hanumaiah, and S. Pepin, Eur. Phys. J. A **19**, 247 (2004).
[13] G. Altarelli, N. Cabibbo, G. Corbo, L. Maiani, and G. Martinelli, Nucl. Phys. **B208**, 365 (1982).
[14] D. Ebert, R. N. Faustov, and V. O. Galkin, Phys. Rev. D **67**, 014027 (2003).
[15] S. N. Gupta, J. M. Johnson, and W. W. Repko, Phys. Rev. D **54**, 2075 (1996).
[16] S. Godfrey, Phys. Rev. D **33**, 1391 (1986).
[17] S. B. Khadkikar and S. K. Gupta, Phys. Lett. **B124**, 523 (1983).
[18] D. S. Hwang, C. S. Kim, and W. Namgung, Phys. Rev. D **53**, 4951 (1996).
[19] J. N. Pandya and P. C. Vinodkumar, Pramana J. Phys. **57**, 821 (2001).
[20] P. C. Vinodkumar, J. N. Pandya, V. M. Bannur, and S. B. Khadkikar, Eur. Phys. J. A **4**, 83 (1999).
[21] A. K. Rai, R. H. Parmar, and P. C. Vinodkumar J. Phys. G **28**, 2275 (2002).

[22] A. K. Rai, J. N. Pandya, and P. C. Vinodkumar, J. Phys. G **31**, 1453 (2005).

[23] A. K. Rai and P. C. Vinodkumar, Pramana J. Phys. **66**, 953 (2006).

[24] A. A. El-Hady, M. A. K. Lodhi, and J. P. Vary, Phys. Rev. D **59**, 094001 (1999).

[25] N. Barmbilla *et al.*, CERN Yellow Report, CERN-2005-005, Geneva: arXive:hep-ph/0412158.

[26] T. Appelquist and H. D. Politzer, Phys. Rev. Lett. **34**, 43 (1975).

[27] R. Barbieri, R. Gatto, and R. Kogerler, Phys. Lett. **B60**, 183 (1976).

[28] R. Barbieri *et al.*, Nucl. Phys. **B154**, 535 (1979).

[29] K. Hagiwara, C. B. Kim, and T. Yosino, Nucl. Phys. **B177**, 461 (1981).

[30] P. B. Mackenzie and G. P. Lepage, Phys. Rev. Lett. **47**, 1244 (1981).

[31] G. T. Bodwin and A. Petrelli, Phys. Rev. D **66**, 094011 (2002).

[32] R. Barbieri, M. Caffo, R. Gatto, and E. Remiddi, Phys. Lett. **B95**, 93 (1980); Nucl. Phys. **B192**, 61 (1981).

[33] G. T. Bodwin, E. Braaten, and G. P. Lepage, Phys. Rev. D **51**, 1125 (1995); [Erratum-*ibid*. **55**, 5853 (1997)].

[34] A. Pineda and J. Soto, Nucl. Phys. B, Proc. Suppl. **64**, 428 (1998).

[35] Nora Brambilla, Dolors Eiras, Antonia Pineda, and Joan Soto, Antonio Vairo, Phys. Rev. D **67**, 034018 (2003).

[36] Nora Brambilla, Antonia Pineda, and Joan Soto, Antonio Vairo, Rev. Mod. Phys. **77**, 1423 (2005).

[37] Chin-Wen Hwang and Zheng-Tao Wei, J. Phys. G **34**, 687 (2007).

[38] H. Y. Cheng, C. Y. Cheung, and C. W. Hwang, Phys. Rev. D **55**, 1159 (1997).

[39] S. M. Ikhdair and Ramazan Sever, Int. J. Mod. Phys. A **19**, 1771 (2004); **20**, 4035 (2005).

[40] L. Motyka and K. Zalewiski, Eur. Phys. J. C **4**, 107 (1998); Z. Phys. C **69**, 343 (1996).

[41] X. Song, J. Phys. G **17**, 49 (1991).

[42] Sterrett J. Collins, T. D. Imbo, B. A. King, and E. C. Martell, Phys. Lett. **B393**, 155 (1997).

[43] S. S. Gershtein, V. V. Kiselev, A. K. Likhoded, and A. V. Tkabladze, Phys. Rev. D **51**, 3613 (1995).

[44] E. J. Eichten and C. Quigg, Phys. Rev. D **49**, 5845 (1994).

[45] S. N. Gupta, S. F. Radford, and W. W. Repko, Phys. Rev. D **26**, 3305 (1982).

[46] R. Van Royen and V. F. Weisskopf, Nuovo Cimento **50**, 617 (1967).

[47] D. S. Hwang and Gwang-Hee Kim, Z. Phys. C **76**, 107 (1997).

[48] E. Braaten and S. Fleming, Phys. Rev. D **52**, 181 (1995).

[49] S. S. Gershtein, hep-ph/9803433 (1998).

[50] L. A. M. Salcedo, Braz. J. Phys. **34**, 297 (2004).

[51] Stephen Godfrey, Phys. Rev. D **70**, 054017 (2004).

[52] F. Abe *et al.* (CDF Collaboration), Phys. Rev. D **58**, 112004 (1998).

[53] Abe *et al.* (Bell Collaboration), Phys. Rev. Lett. **89**, 142001 (2002).

[54] S. F. Radford and W. W. Repko, Phys. Rev. D **75**, 074031 (2007).

[55] K. W. Edwards *et al.* (CLEO Collaboration) Phys. Rev. Lett. **86**, 30 (2001).

[56] G. L. Wang, Phys. Lett. **B633**, 492 (2006).

[57] E. Braaten and J. Lee, Phys. Rev. D **67**, 054007 (2003).

[58] N. Fabiano and G. Pancheri, Eur. Phys. J. C **25**, 421 (2002).

[59] A. Gray, I. Allison, C. T. H. Davies, E. Gulez, G. P. Lepage, J. Shigemitsu, and M. Wingate, Phys. Rev. D **72**, 094507 (2005).

[60] H. Khan and P. Hoodbhoy, Phys. Rev. D **53**, 2534 (1996).